Journal of Systems Engineering and Electronics
Vol. 34, No. 1, February 2023, pp.99 – 116

A multi-UAV deployment method for border patrolling based on Stackelberg game

LEI Xing[1,2], HU Xiaoxuan[1,2], WANG Guoqiang[1,2,3], and LUO He[1,3,*]

1. School of Management, Hefei University of Technology, Hefei 230009, China; 2. Key Laboratory of Process Optimization & Intelligent Decision-making, Ministry of Education, Hefei 230009, China; 3. Engineering Research Center for Intelligent Decision-making & Information Systems Technologies, Ministry of Education, Hefei 230009, China

Abstract: To strengthen border patrol measures, unmanned aerial vehicles (UAVs) are gradually used in many countries to detect illegal entries on borders. However, how to efficiently deploy limited UAVs to patrol on borders of large areas remains challenging. In this paper, we first model the problem of deploying UAVs for border patrol as a Stackelberg game. Two players are considered in this game: The border patrol agency is the leader, who optimizes the patrol path of UAVs to detect the illegal immigrant. The illegal immigrant is the follower, who selects a certain area of the border to pass through at a certain time after observing the leader's strategy. Second, a compact linear programming problem is proposed to tackle the exponential growth of the number of leader's strategies. Third, a method is proposed to reduce the size of the strategy space of the follower. Then, we provide some theoretic results to present the effect of parameters of the model on leader's utilities. Experimental results demonstrate the positive effect of limited starting and ending areas of UAV's patrolling conditions and multiple patrolling altitudes on the leader's utility, and show that the proposed solution outperforms two conventional patrol strategies and has strong robustness.

Keywords: border patrol, unmanned aerial vehicle (UAV), Stackelberg game, compact linear programming, dominated strategy elimination.

DOI: 10.23919/JSEE.2023.000022

1. Introduction

Protecting borders from illegal entry activities is vital to national security [1]. Many countries have built fences, walls, and barriers to enhance the border security. However, such defense measures can play an important role only by effectively scheduling and deploying patrol resources [2,3]. Furthermore, the arbitrariness and unpredictability of illegal cross-border activities, as well as the vast and geographically diversified border areas, have increased the attention to strengthen border patrol measures. Unmanned aerial vehicles (UAVs) are new detection platforms with zero casualties and high flexibility, which can independently complete a given task in different geographical areas [4−6]. At present, the use of UAVs to patrol national borders has gradually become an important border patrol measure in many countries. For example, the United States has expanded its UAV system coverage to the entire southwest border and used UAVs to monitor remote areas [1]. The European Union uses UAVs to enhance the ability to intercept potentially illegal immigrants [7]. However, given the vast area of the border, it is impossible to cover the entire border at all times with limited UAVs. An urgent problem is how to effectively deploy UAVs in vast border areas to better ensure border security.

Recently, Stackelberg game has been used in studying security issues, which models the security problem as a non-cooperative game between the leader and the follower, aims to find an effective strategy for the leader [8]. The unique and attractive feature of the Stackelberg game in modeling security problems is that the leader will first commit a random patrol strategy. The follower makes the optimal choice after observing the leader's strategy. In this model, the leader makes decisions knowing that it will be observed. Therefore, the leader randomizes all possible pure strategies to maximize its own utility. The emphasis of randomization is on generating an unpredictable strategy, because a fixed or patterned strategy will be observed and utilized by the follower. At present, this method has been successfully applied to some practical problems [9−11]. However, the following problem is that the scale of practical problems is huge. The number of pure strategies is extremely large, not to mention the mixed strategies of probability distribution over these pure strategies. Therefore, how to effectively reduce the number of strategies and improve the efficiency of solv-

Manuscript received July 14, 2021.
*Corresponding author.
This work was supported by the National Natural Science Foundation of China (71971075; 71871079), the National Key Research and Development Program of China (2019YFE0110300), the Anhui Provincial Natural Science Foundation (1808085MG213), and the Fundamental Research Funds for the Central Universities (PA2019GDPK0082).

ing the problem should be a new focus.

The problem considered in this paper is that the border patrol agency deploys a certain number of UAVs to patrol the border to detect the potentially illegal immigrants. This deployment is achieved by scheduling the patrol time, patrol area, and patrol altitude of each UAV in a patrol duration. Considering the effect of the surrounding environment on the detection accuracy of equipment carried by UAVs, we assume that the UAV detects the illegal immigrant with a certain probability. In addition, considering the continuity of actual patrols, the UAV is limited in starting and ending its patrol in certain areas. The illegal immigrant can observe the patrol schedule and select a time and area with the minimum probability of being detected to cross the border. In contrast, the border patrol agency aims to maximize such probability.

Although some studies have focused on generating an optimal patrol strategy to protect border security [12,13], the approach that addresses all of above factors simultaneously is still ignored. In addition, unlike the deployment of static resources in the existing border patrol research [14,15], there is an exponential increase in the number of strategies due to temporal and spatial constraints, which introduces huge computational challenges to the problem.

In this paper, first, the problem of deploying UAVs to patrol the border to detect the illegal immigrant is modeled as a Stackelberg game, where the leader uses the time- and space-dependent path of multiple UAVs as its patrol strategy, and the follower uses a continuous period of crossing as its border-crossing strategy. Second, we develop a compact linear programming problem, where the patrol strategies are expressed as flows on graphs. The computational complexity of the enumerating exponential strategy is simplified as solving the optimal solution of linear programming. Third, we propose a method to eliminate the dominated strategies of the follower. The number of strategies of the follower can be reduced to $2/T$ of the original pure strategies, where T is the patrol duration. Then, we provide the conditions on areas where the UAV is limited to starting and ending its patrol to prevent the invalid leader's strategies. Some theoretic results on utilities are stated to provide a preliminary judgment for some cases. Numerical results show that our solution has significantly better quality than the two existing conventional patrol strategies. The limitation on start and end zones ensures the continuity of patrols without much loss of utility and the increasing patrol altitude can increase leader's utility when the detection probability of UAV is not greatly reduced. Additionally, our solution has strong robustness under different perturbations.

The remainder of this paper is structured as follows: Section 2 reviews the literature on the application of security games and briefly introduces the research work related to this issue. Section 3 contains a detailed description of the problem and the mathematical programming formulation. Section 4 introduces the compact linear programming, explains the elimination method of the proposed strategy and provides some theoretical results on utility. Section 5 presents the computational experiment and explains the experimental results. Section 6 concludes the contributions of this paper and discusses future work.

2. Related work

Security issues are ubiquitous in real life. These issues have attracted people's attention, especially those related to the security of important places of national economy and politics. The key of the security problem is how to effectively deploy limited defense resources on vast area to patrol to prevent possible attacks [16−18]. Fixed or patterned patrol methods are easily observed by the attacker, who attacks the intervals between patrols. The Stackelberg game was first used in security problems and solved the difficulties of generating a random patrol strategy. Team Core, a team of researchers at the University of Southern California, has been working in this area. They first successfully deployed the assistant for randomized monitoring over routes (ARMORs) [9] at the Los Angeles International Airport to solve the problems of checkpoint selection on the way to the airport. Then, intelligent randomization in scheduling (IRIS) [10], game-theoretic unpredictable and randomly deployed security (GUARDS) [11], and port resilience operational/tactical enforcement to combat terrorism (PROTECT) [19] were successively developed for the Federal Air Marshals, the United States Transportation Safety Administration and the Boston Port. Unlike ARMOR and IRIS, which focus on specialized customized applications, GUARDS and PROTECT are used in larger scale deployments, which further create computational challenges in the security game [20,21]. Similarly, the deployment of resources on the border is a problem of deploying the limited resources to a wide range of areas.

Border security is one of the most important security problems, which is vital to homeland security and has attracted the attention of many researchers. Canbolat et al. [22] discussed the optimal location of emergency facilities in the presence of a limited set of points along the border. Karabulut et al. [14] modeled the interaction between the border surveillance agency and the intruder as a Stackelberg game. The agency deploys a set of sensors to achieve coverage intensity to increase the possibility of detection, while the intruder selects a path that minimizes exposure or maximizes damage to the sensors. Recent research is about the optimal deployment of security resources between different precincts in a border patrol problem [13]. The core of these problems lies in the exponential growth of the number of deployment schemes with the increase in spatial scale.

Unlike the deployment of the above static resources, UAVs are mobile, so the static one-off deployment becomes dynamically covered. UAV patrol strategies include both temporal and spatial dimensions, which introduces great computational challenges to deploying UAVs on borders. An effective method to address the considerable strategy space is to reduce the scale of the game through effective technology [23]. Yin et al. [24] introduced a directed graph to transform the patrol strategy form, which greatly reduces the number of variables in the original problem. This transformation of strategy in the form of a graph exists in many patrol problems, such as determining the optimal patrol path for mobile robots [25] and discussing the value and optimal patrol strategy of patrolling games for arbitrary graphs [26,27] and line graphs [28]. These studies discuss how to reduce the scale of the game from the patrol side, i.e., to solve the problem of the large scale of the patrol strategy. However, there are many attacker strategies in many practical problems, which directly affect the efficiency of solving the problem.

As a new type of patrol platform, UAVs have been gradually applied to the border patrol process [29]. Earlier research constructed a UAV system based on a hierarchical control architecture to manage multiple UAVs to perform border patrol tasks [30]. A recent paper proposed a detection method to support the UAV patrol and surveillance at the border and analyzed the problem of target recognition when UAVs are used for high-altitude patrols in border and forest areas [31]. Another recent research is about how to overcome the limited time of UAVs in border patrol [32]. Due to information acquisition or equipment factors, there are certain uncertainties when UAVs perform tasks [33–35]. When UAVs are used to perform border patrol tasks, considering the accuracy of the equipment carried by UAVs in practice, there is a degree of uncertainty in the patrol process. The resulting uncertainties are reflected in the probability of UAVs detecting the illegal immigrant in each patrol area. Similar research on UAV detection probability includes introducing a variable resolution sensing model to address the problem of variable probability of UAV detection, which is suitable for the online patrol with uniform grids [36]. On this basis, how heterogeneous UAVs cooperate in patrolling designated areas was analyzed, and different sensor models were introduced to predict the optimal patrol team size and performance configuration [37].

Despite efforts to enhance border security, an optimal patrol strategy considering the decision-making effect of both patroller and illegal immigrant, limited UAVs, the patrol altitude of UAVs and limited start and end areas simultaneously remains elusive. To provide an effective patrol strategy, this paper first constructs a Stackelberg game for the border security problem. However, the extensive number of strategies makes it difficult to solve the game [38,39]. Therefore, this paper reduces the scale of the game from two perspectives. First, it transforms the leader's strategies to a compact form to reduce the model variables. Then, it uses the concept of dominated strategy to eliminate the follower's strategies. In addition, the impact of the actual environment on detection is considered, which makes the problem more relevant to real patrols. To the best of our knowledge, this is the first work that focuses on the deployment of UAVs to patrol the border considering the strategies of the illegal immigration and multiple patrol altitudes.

3. Stackelberg game model

In this section, we introduce the problem, which is modeled as a Stackelberg game between a leader and a follower. The leader deploys a group of UAVs on the border to detect illegal immigrants. Its strategy is a patrol path on the border within the flight time of the UAVs. Since the border is too long to be handled with continuous variables, we divide the border into a group of small zones. The time is discretized into a series of time points. The intervals between every two consecutive time points are equal [40]. When the UAV patrols in a zone, it can fully cover the zone. The UAV can always cover the current zone or move to adjacent zones. In addition, the UAV is limited in starting and ending its patrol path in certain zones. It can patrol at certain altitudes with different numbers of covered zones. Fig. 1 illustrates a possible patrol path of three UAVs between two consecutive time points. The follower can observe the leader's strategy and subsequently select a zone of the border to pass through for some time. The UAVs transmit images to border staff in real time, and the staff intercept the follower after detection. Therefore, we consider only the optimal deployment of UAVs here. If the follower is not detected and successfully crosses the border, it is easy for him or her to escape by camouflage or other means.

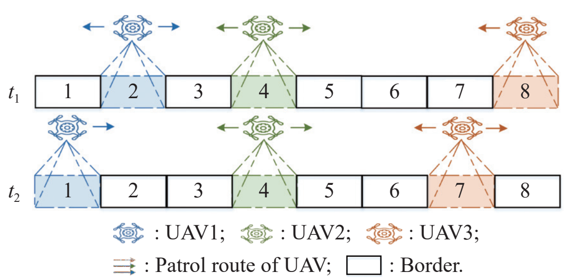

Fig. 1 Possible patrol path of three UAVs at a certain altitude between two consecutive time points

3.1 Border

We assume that border R contains r zones, $R=\{1,2,\cdots,r\}$. For a zone $i\in R$, its adjacent zones are denoted by $N(i)$, and $i\in N(i)$. Then, the patrol duration t is discretized into T time points, $t=\{t_1,t_2,\cdots,t_T\}$, and the interval between adjacent time points is a time step. Assuming that the UAV moves only at time points and moves to its adjacent zone, the time required for the UAV to move from one zone to its adjacent zone is a time step. Furthermore, a directed graph $G=(V,E)$ is constructed to represent the players' strategies, where a vertex $v=(i,t_k)$ includes zone i and time point t_k. There is an edge e between vertices $v'=(i',t_{k'})$ and $v''=(i'',t_{k''})$ when $i''\in N(i')$ and $k''=k'+1$.

Fig. 2(a) shows an example of the constructed directed graph. The edge between vertices $(3,t_2)$ and $(2,t_3)$ indicates that the UAV moves from Zone 3 at time point t_2 and arrives at Zone 2 at time point t_3. The edges between vertices $(3,t_2)$ and $(3,t_3)$ indicate that the UAV patrols in Zone 3 between time points t_2 and t_3.

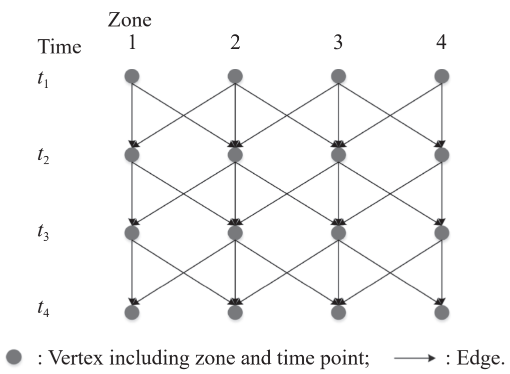

(a) Directed graph G with r=4 and T=4

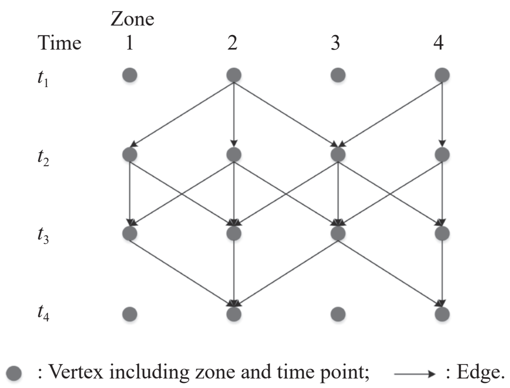

(b) Directed graph G with r=4, T=4, and R={2, 4}

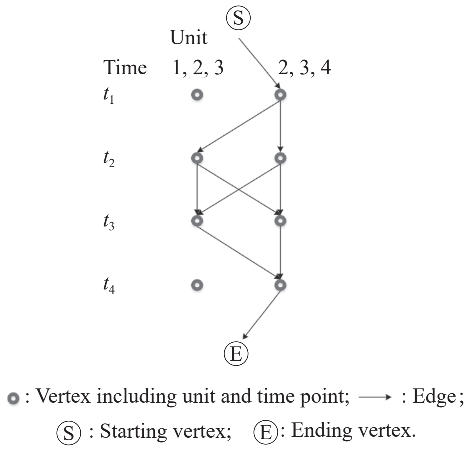

(c) Directed graph G_h with r=4, T=4, λ_h=3, and R={2, 4}

Fig. 2 Examples of directed graph

3.2 Leader strategies

The leader determines the patrol path of each UAV. We assume that the leader has m homogeneous UAVs. Let $R_d\subseteq R$ be the zones where the UAV can start and end its patrol. Specifically, when $R_d=R$, i.e., the UAV can start and end its patrol in any zone. When $R_d\subset R$, the UAV is limited to starting and ending its patrol in the zone in R_d. Fig. 2(b) illustrates a possible R_d on graph G.

Then, let H be the patrol altitudes of UAV. The number of zones covered by the UAVs at altitude $h\in H$ is λ_h. Let j_h be the patrol unit at altitude h, which contains λ_h zones. $R_h=\left\{j_h^1,j_h^2,\cdots,j_h^{|R_h|}\right\}$ is the set of patrol units at altitude h. We use j_{h_0} to represent the zone with the smallest number in patrol unit j_h, $j_{h_0}=1,2,\cdots,r+1-\lambda_h$, and $j_h=\{j_{h_0},j_{h_0}+1,\cdots,j_{h_0}+\lambda_h-1\}$. Specifically, when $|H|=1$, UAVs are limited to patrolling at a certain altitude.

Furthermore, we construct a group of directed graphs $G'=\{G_h\}_{h\in H}$ to represent the patrol path of UAVs at different altitudes. For G_h, its vertex $v_h=(j_h,t_k)$ includes patrol unit j_h and time point t_k ($k\in\{1,2,\cdots,T\}$). There is an edge e between vertices $v'_h=(j'_h,t_{k'})$ and $v''_h=(j''_h,t_{k''})$ when $j''_{h_0}\in N\left(j'_{h_0}\right)$ and $k''=k'+1$. Since the UAV can patrol at any altitude in H, we add a set of virtual starting vertices $S=\{S_1,S_2,\cdots,S_{|H|}\}$ to $G'=\{G_h\}_{h\in H}$. For $S_h\in S$, we add an edge between vertex S_h and $(j_h,t_1)(\forall j_{h_0}\in R_d)$. Similarly, we add a set of virtual ending vertices $E=\{E_1,E_2,\cdots,E_{|H|}\}$ to $G'=\{G_h\}_{h\in H}$. For $E_h\in E$, we add an edge between vertex E_h and $(j_h,t_T)(\forall j_{h_0}\in R_d)$. Specifically, when $|H|=1$ and $\lambda_h=1$, $G'=G_h=G$. Fig. 2(c) illustrates a possible directed graph G_h.

Therefore, a patrol path of UAV $w\in W=\{1,2,\cdots,m\}$ is a path between S_h and E_h on graph G_h, i.e., $d_w=$

$(S_h, (j_h, t_k), E_h)$, $j_h \in R_h, k \in \{1, 2, \cdots, T\}$. Fig. 3(a) illustrates a possible path of UAV on G_h. A pure strategy of the leader is m paths of m UAVs, i.e., $\boldsymbol{d} = (d_w)_{w \in W}$. The probability distribution $\boldsymbol{x} = (x_d)_{d \in D}$ of all pure strategies is a mixed strategy of the leader, where x_d is the probability of selecting strategy $\boldsymbol{d}$, $0 \leqslant x_d \leqslant 1$ and $\sum_{d=1}^{|D|} x_d = 1$.

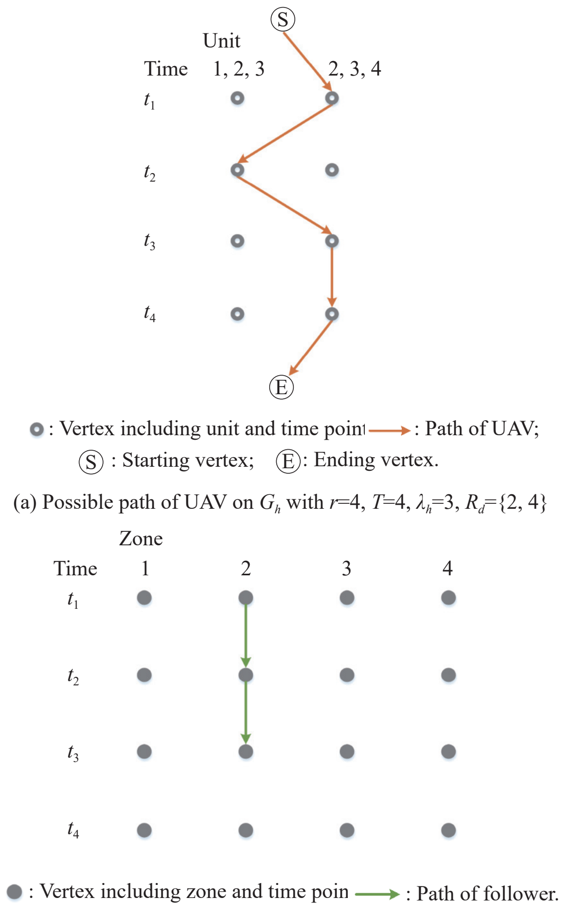

(a) Possible path of UAV on G_h with r=4, T=4, λ_h=3, R_d={2, 4}

(b) Possible path of the follower on G

Fig. 3 Examples of path of the UAV and the follower

3.3 Follower strategies

We define a pure strategy of the follower as a path $a = \langle (i, t_k), (i, t_{k+1}), \cdots, (i, t_{k+l}) \rangle$ on G, i.e., the follower passes through zone i within l time steps between time points $t_k (k \geqslant 1)$ and t_{k+l} $(k + l \leqslant T)$. On graph G, a pure strategy of the follower is any path that connects the same zone, thus the number of pure strategies of the follower is $C_T^2 \cdot r = (T(T-1)/2) \cdot r$. Fig. 3(b) illustrates a possible path of the follower on G. Similar to the relevant research in security games, this paper restricts the follower's strategy to a pure strategy [41].

3.4 Utilities and equilibrium

When the zone of one vertex in the strategy selected by the follower is included in the unit of one vertex of the UAV's patrol path and the time points of two vertices are identical, the follower may be found by the UAV. We call these types of vertices coincident vertices. Given the pure strategy $\boldsymbol{d} = (d_w)_{w \in W}$ of the leader and pure strategy a of the follower, the coincident vertices in the patrol path of UAV w are

$$V_{(w,a)} = \{(j_h, t_k) | (j_h, t_k) \in d_w, \exists (i, t_k) \in a \text{ s.t. } i \in j_h\}.$$

Let $\delta(v_h)$ be the detection probability of the UAV at v_h, $\delta(v_h) \in (0, 1)$. Then, let $p(w, a)$ be the probability of UAV w detecting the follower, which can be defined as

$$1 - p(w, a) = \prod_{v \in V_{(w,a)}} (1 - \delta(v_h)). \tag{1}$$

Assuming that each UAV is independent, given a pair of strategies $(\boldsymbol{d}, a)$, the probability of the follower being detected by the leader $p(\boldsymbol{d}, a)$ satisfies

$$1 - p(\boldsymbol{d}, a) = \prod_{w=1}^{m} (1 - p(w, a)). \tag{2}$$

The follower expects to maximize the probability of being undetected by the leader. Based on (1) and (2), given a pair of strategies $(\boldsymbol{d}, a)$, the utility of the follower is

$$U_a(\boldsymbol{d}, a) = \prod_{w=1}^{m} \prod_{v \in V_{(w,a)}} (1 - \delta(v_h)). \tag{3}$$

The leader expects to minimize the probability of not detecting the follower. Let the utility of the leader be $-U_a(\boldsymbol{d}, a)$. Maximizing the utility of the leader means minimizing the probability of not detecting the follower. Therefore, our game is a zero-sum game. Given the mixed strategy $\boldsymbol{x} = (x_d)_{d \in D}$ of the leader and pure strategy a of the follower, the expected utility of the follower is

$$U_a(\boldsymbol{x}, a) = \sum_d x_d U_a(\boldsymbol{d}, a),$$

and the expected utility of the leader is

$$U_d(\boldsymbol{x}, a) = -U_a(\boldsymbol{x}, a).$$

Our goal is to find the optimal strategy of the leader, which is to find the strong Stackelberg equilibrium in the game. Given the zero-sum setting, the strong Stackelberg equilibrium is equivalent to maximizing the leader's utility when the follower responds with its optimal strategy. Let $\boldsymbol{X}$ and A be the strategy space of the leader and follower, respectively. A pair of strategies $\langle \boldsymbol{x}, g \rangle$ comprises an equilibrium when it satisfies

$$\begin{cases} U_d(\boldsymbol{x}, g(\boldsymbol{x})) \geqslant U_d(\boldsymbol{x}', g(\boldsymbol{x}')), & \forall \boldsymbol{x}' \in \boldsymbol{X} \\ U_a(\boldsymbol{x}, g(\boldsymbol{x})) \geqslant U_a(\boldsymbol{x}, g'(\boldsymbol{x})), & \forall g'(\boldsymbol{x}) \in A \end{cases}$$

where $g(\boldsymbol{x})$ is the optimal response function of the follower. In the setting of a bi-level programming problem, the first objective function and its appropriate constraints constitute the upper-level optimization problem. The lower-level optimization problem takes the appropriate objective function and constraints as the nesting problem of the upper-level optimization problem, which is consistent with the fact that in the Stackelberg game, the leader first promises a mixed strategy, and the follower subsequently makes decisions after observation.

Therefore, the above conditions can be formulated as bi-level programming problems:

$$\max_{\boldsymbol{x},\boldsymbol{y}} U_d(\boldsymbol{x},\boldsymbol{y})$$

$$\text{s.t.} \begin{cases} \sum_{d=1}^{|D|} x_d = 1 \\ \boldsymbol{x} \in [0,1]^{|D|} \end{cases},$$

$$\max_{\boldsymbol{y}} U_a(\boldsymbol{x},\boldsymbol{y})$$

$$\text{s.t.} \begin{cases} \sum_{a=1}^{|A|} y_a = 1 \\ \boldsymbol{y} \in \{0,1\}^{|A|} \end{cases},$$

where y_a is the probability of selecting strategy a. In this bi-level programming problem, the leader's optimization problem is the upper-level optimization problem, and the follower's objective function and constraints are the nested problems of the leader's optimization problem.

4. Solution method

In this section, we mainly discuss how to solve the problem of the rapid increase in number of pure strategies of the leader and follower with the scale of the game. Some theoretic results are stated to provide preliminary judgments on the leaders' strategies and utilities.

4.1 Linear program formulation

With increasing game scale and number of UAV patrol altitudes, the number of leader's pure strategies exponentially increases. To solve the computational challenge, the mixed strategies of the leader are compactly represented by marginal coverage:

$$f_h(v_h) = \sum_d x_d d(v_h)$$

where $d(v_h)$ is the number of UAVs covering vertex v_h in pure strategy $\boldsymbol{d}$. Given mixed strategy $\boldsymbol{x}$ of the leader, the corresponding marginal coverage vector $\boldsymbol{f}=\{f_h(v_h)\}_{v_h \in V_h, h \in H}$ and pure strategy a of the follower, the expected utility of the follower is

$$U_a(\boldsymbol{f},a) = \prod_{h \in H} \prod_{v_h \in V_h(a)} (1-\delta(v_h))^{f_h(v_h)} \tag{4}$$

where

$$V_h(a) = \left\{ (j_h,t_k) \,\middle|\, (j_h,t_k) \in G_h, \exists (i,t_k) \in a \text{ s.t. } i \in j_h \right\}.$$

Now, we construct the optimization linear programming problem using compact representation (CRLP) to solve the optimal marginal coverage:

$$\max_{\boldsymbol{f}} U_d \tag{5}$$

subject to

$$U_d \leqslant -U_a(\boldsymbol{f},a), \ \forall a \in A \tag{6}$$

$$f_h(v_h) = \sum_{(v_h, v''_h) \in G_h} z_h(v_h, v''_h), \quad \forall v_h \in G_h; \forall G_h, \tag{7}$$

$$f_h(v_h) = \sum_{(v'_h, v_h) \in G_h} z_h(v'_h, v_h), \quad \forall v_h \in G_h; \forall G_h, \tag{8}$$

$$\sum_{S_h \in S} \sum_{j_h \in R_h} z_h(S_h, (j_h, t_1)) = m, \tag{9}$$

$$\sum_{E_h \in E} \sum_{j_h \in R_h} z_h((j_h, t_T), B_h) = m, \tag{10}$$

$$z_h(v_h, v_h') \geqslant 0, \quad \forall (v_h, v_h') \in G_h; \forall G_h. \tag{11}$$

Constraint (6) indicates that the follower will select a strategy that maximizes its utility, i.e., a strategy that minimizes the utility of the leader. Constraints (7) and (8) are constraints of flow conservation. Constraints (9) and (10) constrain the total number of UAVs that start and end patrols to m, and constraint (11) represents the range of variables in the model.

Recall that the follower aims to maximize $U_a(\boldsymbol{f},a)$. Since the natural logarithm function $\ln x (x>0)$ is a strictly increasing function and $0<\delta(v_h)<1$, i.e., $1-\delta(v_h)>0$, maximizing U_a is equivalent to maximizing $\ln U_a$. Thus,

$$U_a(\boldsymbol{f},a) = \prod_{h \in H} \prod_{v_h \in V_h(a)} (1-\delta(v_h))^{f_h(v_h)},$$

$$\ln U_a(\boldsymbol{f},a) = \ln \left\{ \prod_{h \in H} \prod_{v_h \in V_h(a)} (1-\delta(v_h))^{f_h(v_h)} \right\} =$$

$$\sum_{h \in H} \ln \left\{ \prod_{v_h \in V_h(a)} (1-\delta(v_h))^{f_h(v_h)} \right\} =$$

$$\sum_{h \in H} \sum_{v_h \in V_h(a)} \ln (1-\delta(v_h))^{f_h(v_h)} =$$

$$\sum_{h \in H} \sum_{v_h \in V_h(a)} f_h(v_h) \ln (1-\delta(v_h)).$$

Constraint (4) is transformed into

$$U_d' \leqslant - \left\{ \sum_{h \in H} \sum_{v_h \in V_h(a)} f_h(v_h) \ln (1-\delta(v_h)) \right\}, \ \forall a \in A. \tag{12}$$

The objective function is

$$\max_{f} U_d{}', \tag{13}$$

and

$$U_d = -\exp(-U_d'). \tag{14}$$

Therefore, solving the optimal marginal coverage is transformed into solving the linear programming problem. After identifying the optimal solution of the linear problem, the optimal utility of the leader can be obtained by (13). According to [24], the mixed strategy of the leader with identical utility to the optimal coverage can be constructed in polynomial time.

4.2 Strategy elimination method

Recall that the number of pure strategies of the follower is $C_T^2 \cdot r = (T(T-1)/2) \cdot r$, which geometrically increases with time duration T and zones r. Thus, we provide the dominated strategy elimination method (DS-EM) to reduce the number of strategies as follows.

Definition 1 (Weakly dominated strategy) A strategy $a \in A$ of the follower is weakly dominated if $\forall \boldsymbol{f}$,

$$\exists a' \in A \backslash \{a\} : U_a(\boldsymbol{f}, a) \leqslant U_a(\boldsymbol{f}, a').$$

The follower does not select a weakly dominated strategy because the utility will not be higher.

Lemma 1 Considering l pure strategies of the follower,

$$a_1^i = \langle (i,t_k),(i,t_{k+1})\rangle,\ a_2^i = \langle (i,t_k),(i,t_{k+1}),(i,t_{k+2})\rangle, \cdots, \\ a_l^i = \langle (i,t_k),(i,t_{k+1}),\cdots,(i,t_{k+l})\rangle$$

where $k \geqslant 1$ and $k+l \leqslant T$. $a_l^i = \langle (i,t_k),(i,t_{k+1}),\cdots,(i,t_{k+l})\rangle$ is a pure strategy with time step l related to zone i. Given the marginal coverage vector $\boldsymbol{f} = \{f_h(v_h)\}_{v_h \in V_h, h\in H}$ of the leader, the relationship between the follower's utility $U_a(\boldsymbol{f}, a_1^i), U_a(\boldsymbol{f}, a_2^i), \cdots, U_a(\boldsymbol{f}, a_l^i)$ corresponding to l strategies satisfies:

$$U_a\left(\boldsymbol{f}, a_1^i\right) \geqslant U_a\left(\boldsymbol{f}, a_2^i\right) \geqslant \cdots \geqslant U_a\left(\boldsymbol{f}, a_l^i\right).$$

Proof Let

$$a_1^i = \langle (i,t_k),(i,t_{k+1})\rangle,\ a_2^i = \langle (i,t_k),(i,t_{k+1}),(i,t_{k+2})\rangle, \cdots, \\ a_l^i = \langle (i,t_k),(i,t_{k+1}),\cdots,(i,t_{k+l})\rangle$$

be l pure strategies of the follower. For an arbitrary marginal coverage vector $\boldsymbol{f} = \{f_h(v_h)\}_{v_h \in V_h, h\in H}$ of the leader, the utility of the follower corresponding to strategy a_1^i is

$$U_a(\boldsymbol{f}, a_1^i) = \prod_{h\in H} \prod_{j_h \in v_h : i \in j_h} (1-\delta(j_h,t_k))^{f_h(j_h,t_k)} \cdot \\ (1-\delta(j_h,t_{k+1}))^{f_h(j_h,t_{k+1})}.$$

The utility of the follower that corresponds to strategy a_2^i is

$$U_a(\boldsymbol{f}, a_2^i) = \prod_{h\in H} \prod_{j_h \in v_h : i \in j_h} (1-\delta(j_h,t_k))^{f_h(j_h,t_k)} \cdot \\ (1-\delta(j_h,t_{k+1}))^{f_h(j_h,t_{k+1})} \cdot (1-\delta(j_h,t_{k+2}))^{f_h(j_h,t_{k+2})}.$$

The value range of the exponential function $a^x (0 < a < 1)$ is $0 < a^x \leqslant 1$ when $x \geqslant 0$. In addition, $0 < \delta(v_h) < 1$; obviously, $0 < 1-\delta(v_h) < 1$. Based on constraints (5) and (6), $f(v) \geqslant 0$.

Thus, $0 < (1-\delta(j_h,t_{k+2}))^{f_h(j_h,t_{k+2})} \leqslant 1$. Therefore, $U_a(\boldsymbol{f}, a_1^i) \geqslant U_a(\boldsymbol{f}, a_2^i)$.

Similarly,

$$U_a\left(\boldsymbol{f}, a_2^i\right) \geqslant U_a\left(\boldsymbol{f}, a_3^i\right), U_a\left(\boldsymbol{f}, a_3^i\right) \geqslant U_a\left(\boldsymbol{f}, a_4^i\right), \cdots, \\ U_a\left(\boldsymbol{f}, a_{l-1}^i\right) \geqslant U_a\left(\boldsymbol{f}, a_l^i\right).$$

Therefore,

$$U_a\left(\boldsymbol{f}, a_1^i\right) \geqslant U_a\left(\boldsymbol{f}, a_2^i\right) \geqslant \cdots \geqslant U_a\left(\boldsymbol{f}, a_l^i\right). \qquad \square$$

Theorem 1 For the same zone i, the pure strategy of the follower whose time step is larger than 1 is the weakly dominated strategy of the pure strategy of the follower whose time step is 1.

Proof Lemma 1 shows that in the same zone i, for any given marginal coverage vector of the leader, the utility of the strategy with a time step larger than 1 is always less than or equal to that of the strategy with time step 1. Definition 1 shows that the pure strategy of the follower with a time step larger than 1 is the weakly dominated strategy of the pure strategy of the follower with time step 1. □

According to Theorem 1, we can eliminate the pure strategy of the follower whose time step is larger than 1. After elimination, the strategy space of the follower contains only the pure strategy with time step 1. The number of pure strategies is reduced from $(T(T-1)/2) \cdot r$ to $(T-1) \cdot r$. With the DS-EM, we reduce the number of strategies of the follower to $2/T$ of the original pure strategies.

4.3 Theoretic results

In this subsection, we present some conditions on the start and end zones to provide effective strategies of the leader. Additionally, some general properties of the leader's utility are stated.

4.3.1 Conditions for effective leader's strategies

We find that with the limitation of the start and end zones, the vertices that correspond to the zones outside the set of start and end zones are not patrolled at some time points. If some zones are not patrolled at two or more continuous time points, the follower will cross the border through these zones without being detected. In these cases, the leader's strategies are invalid. We now make certain conditions for the start and end zones to prevent the invalid leader's strategies.

Lemma 2 For R_d, suppose that the following conditions hold:

(i) At least one of Zones 1 and 2 should be the start and end zones, i.e., $1 \in R_d$ or $2 \in R_d$.

(ii) There must be a start zone at most two zones apart, i.e., if $1 \in R_d$, then $4 \in R_d$, $7 \in R_d$, etc.

(iii) At least one of zones $r-1$ and r should be the start and end zones, i.e., $r-1 \in R_d$ or $r \in R_d$.

Then, there are no invalid leader's strategies with the limitations of the start and end zones.

Proof If Zones 1 and 2 are not the start and end zones, there is no UAV patrol in Zone 1 at time points t_1, t_2, t_{T-1}, and t_T because the adjacent zones of Zone 1 are Zone 1 and Zone 2. Only the UAV starts patrolling from Zone 1, Zone 2 can arrive at Zone 1 at time point t_2. To arrive at Zone 1 at time point t_T, the UAV must arrive at Zone 1 or Zone 2 at time point t_{T-1}. Therefore, at least one of Zone 1 and Zone 2 should be the start and end zones. Similarly, at least one of $r-1$ and r should be start and end zones. If the nearest start zones are separated by more than two zones, some zones will not be patrolled at consecutive time points. For example, if Zone 1 and subsequently Zone 5 are start zones, then Zone 3 will not be covered at time points t_1, t_2, t_{T-1}, and t_T. The reason is that at two consecutive time points, the UAV can move only between adjacent zones. Therefore, the start zones must be at most two zones apart; otherwise, some zones will not be covered at consecutive time points. □

Theorem 2 To guarantee the effectiveness of the leader's strategies, the number of start and end zones satisfies:

$$|R_d| \geqslant \left\lceil \frac{r}{3} \right\rceil.$$

Proof Lemma 1 shows that to ensure that there are no invalid leader's strategies, there must be a start zone at most every two zones. When r is a multiple of 3, then $|R_d|$ satisfies $|R_d| \geqslant r/3$; otherwise, $|R_d|$ satisfies $|R_d| \geqslant \lceil r/3 \rceil$.

Therefore, $|R_d|$ satisfies $|R_d| \geqslant \dfrac{r}{3}$. □

4.3.2 General properties of the leader's utilities

When analyzing the effect of the patrol duration and number of UAVs on the leader's utilities, we find some interesting phenomena. We now show the general properties of the leader's utilities in some cases.

Theorem 3 Given graphs G^1 and G^2, suppose that the following conditions hold:

(i) $R^1 = R^2 = R_d^1 = R_d^2$.

(ii) $T^1 < T^2$.

(iii) The detection probability of each vertex at the first T^1 time points on G^2 is identical to that of the corresponding vertex on G^1.

Then the optimal utility of the leader of two digraphs satisfies

$$U_d^{1^*} \geqslant U_d^{2^*}.$$

Proof Let $\boldsymbol{f}^{1^*}$ and $\boldsymbol{f}^{2^*}$ be optimal marginal coverage on G^1 and G^2, respectively; $g(\boldsymbol{f}^{1^*})$ and $g(\boldsymbol{f}^{2^*})$ are the follower's optimal strategies on G^1 and G^2, respectively. According to the definition of the strong Stackelberg equilibrium, the utilities of the leader and follower on G^1 satisfy

$$\begin{cases} U_d^1\left(\boldsymbol{f}^{1^*}, g\left(\boldsymbol{f}^{1^*}\right)\right) \geqslant U_d^1\left(\boldsymbol{f}^1, g\left(\boldsymbol{f}^1\right)\right), \ \forall \boldsymbol{f}^1 \in \boldsymbol{F}^1 \\ U_a^1\left(\boldsymbol{f}^{1^*}, g\left(\boldsymbol{f}^{1^*}\right)\right) \geqslant U_a^1\left(\boldsymbol{f}^1, a\right), \ \forall a \in A^1 \end{cases}.$$

Since G^1 is a subgraph of G^2, the strategy space of the follower satisfies $A^1 \subset A^2$. Then, the optimal strategy of the follower on G^2 satisfies

$$g\left(\boldsymbol{f}^{2^*}\right) = \arg\max_a \left\{ U_a\left(\boldsymbol{f}^{2^*}, a\right) : a \in \left\{ g\left(\boldsymbol{f}^{1^*}\right), A^2 - A^1 \right\} \right\}.$$

Thus, the utility of the follower satisfies

$$U_a^2(\boldsymbol{f}^{2^*}, g\left(\boldsymbol{f}^{2^*}\right)) \geqslant U_a^1\left(\boldsymbol{f}^{1^*}, g\left(\boldsymbol{f}^{1^*}\right)\right).$$

Since the utility of the leader and follower satisfies

$$\begin{cases} U_d = -U_a \\ U_d^2\left(\boldsymbol{f}^{2^*}, g\left(\boldsymbol{f}^{2^*}\right)\right) \leqslant U_d^1\left(\boldsymbol{f}^{1^*}, g\left(\boldsymbol{f}^{1^*}\right)\right) \end{cases}.$$

Therefore, $U_d^{1^*} \geqslant U_d^{2^*}$. □

In actual planning, the patrol duration is a key factor when making a decision. The above result can provide a preliminary judgment for the decision maker. The leader's utility may decrease if he plans a long-span patrol when the detection probability greatly varies among different time spans, such as the weather being fine or overcast. The reason is that there is no accurate information about how many time points of the leader's strategy are observed by the follower. However, planning a strategy for a short duration of time may result in a lack of coherence among the strategies. The end zone of the last patrol may not be the start zone of the next patrol. Thus, there may be movement cost of UAVs.

When other conditions are fixed, with increasing number of UAVs, the leader's utilities will increase. However, what is the relationship between the leader's utilities under different numbers of UAVs? We now present the relationship to provide a preliminary judgment for some cases.

Lemma 3 Let $\boldsymbol{f}^{1^*}$ and $\boldsymbol{f}^{m^*}$ be the optimal marginal coverage on G when the number of UAVs is 1 and m, respectively. Then,

$$\boldsymbol{f}^{m^*} = m\boldsymbol{f}^{1^*}.$$

Proof The optimal solution of the linear programming problem can be expressed as $\boldsymbol{X}^* = \boldsymbol{B}^{-1}\boldsymbol{b}$, where $\boldsymbol{B}$ is the optimal basis linear programming problem, and $\boldsymbol{b}$ is the constant term. In CRLP, the constant term of CRLP is $[0,0,\cdots,0,m,m,\cdots,m]^{\mathrm{T}}$.

Let $\boldsymbol{X}^*=\boldsymbol{B}^{-1}\boldsymbol{b}$ be the optimal solution of CRLP when $\boldsymbol{b}=[0,0,\cdots,0,1,1,\cdots,1]^{\mathrm{T}}$, and let $\boldsymbol{X}'$ be the solution of CRLP when $\boldsymbol{b}'=[0,0,\cdots,0,m,m,\cdots,m]^{\mathrm{T}}$.

Thus $\boldsymbol{b}'=m\boldsymbol{b}$. Hence, the solution of CRLP when $\boldsymbol{b}'=[0,0,\cdots,0,m,m,\cdots,m]^{\mathrm{T}}$ satisfies $\boldsymbol{X}'=m\boldsymbol{B}^{-1}\boldsymbol{b}=m\boldsymbol{X}$. Since the optimal solution of CRLP satisfies $\boldsymbol{X}^*=\boldsymbol{B}^{-1}\boldsymbol{b}\geqslant 0$, $\boldsymbol{X}'\geqslant 0$, the test number remains unchanged and the optimal basis remains unchanged. Then, $\boldsymbol{X}'$ is the optimal solution of CRLP when $\boldsymbol{b}'=[0,0,\cdots,0,m,m,\cdots,m]^{\mathrm{T}}$. Let $\boldsymbol{f}^{1^*}$ and $\boldsymbol{f}^{m^*}$ be the optimal marginal coverage on G when the number of UAVs is 1 and m, respectively. Therefore, $\boldsymbol{f}^{m^*}=m\boldsymbol{f}^{1^*}$. □

Theorem 4 Let $U_d^{1^*}$ and $U_d^{m^*}$ be the optimal utility on G when the number of UAVs is 1 and m, respectively. Then,

$$U_d^{m^*}=-\left(U_d^{1^*}\right)^m.$$

Proof Let $\boldsymbol{f}^{m^*}$ be the optimal marginal coverage on G when the number of UAVs is m. For $\forall a\in A$, the utility of the follower is

$$U_a\left(\boldsymbol{f}^{m^*},a\right)=\prod_{v\in a}(1-\delta(v))^{f^{m^*}(v)}.$$

According to Lemma 4, $\boldsymbol{f}^{m^*}=m\boldsymbol{f}^{1^*}$. Then,

$$U_a(\boldsymbol{f}^{m^*},a)=\prod_{v\in a}(1-\delta(v))^{f^{m^*}(v)}=\prod_{v\in a}(1-\delta(v))^{mf^{1^*}(v)}=\left\{\prod_{v\in a}(1-\delta(v))^{f^{1^*}(v)}\right\}^m=mU_a(\boldsymbol{f}^{1^*},a).$$

The utility of the leader and follower satisfies $U_d=-U_a$. Therefore, $U_d^{m^*}=-(U_d^{1^*})^m$. □

The number of UAVs used in real patrols is also a major concern for decision makers, since it is directly related to costs. The above findings can provide decision makers with an intuitive result about the relationship between the utilities and the number of UAVs.

5. Computational experiment

In this section, we first present the instances. Based on these instances, we analyze and evaluate the performance of the proposed method from three aspects. CRLP is programmed in the C++ language and solved by CPLEX (version 12.7.1). All experiments are run on 64-bit computers with 8.0 GB RAM and a CPU at 1.80 GHz.

5.1 General settings

5.1.1 Instance sets

We generate three test sets of 90 problem instances and conduct experiments on these instances to investigate the effect of the number of zones, UAVs, time points and detection probability. The three test sets are named Set A, Set B, and Set C, and each of them consists of 30 problem instances and has 200−1 000 zones and 6−36 time points. For each instance, we present the results when the number of UAVs is 5, 10, 15, and 20. UAVs can patrol at low, medium and high altitudes. The number of zones covered by the UAVs at the three altitudes is fixed to 1, 2, and 3. The start and end zones are selected according to the conditions in Subsection 4.3. The detection probabilities of the three test sets when the UAVs patrol at low altitudes are randomly generated in [0.4, 0.6), [0.6, 0.8), and [0.8, 1). The three value ranges represent a low detection probability, medium detection probability and high detection probability, respectively. In all instances, the detection probability of UAVs at the middle altitude and high altitude are 0.75 times and 0.6 times of the detection probability at the low altitude. The two values are determined through several sets of experiments which based on practical surveys.

5.1.2 Experimental setting

To illustrate the effect of start and end zones and various patrol altitudes on leader utilities and the scalability of DS-EM, we compare the results between four CRLPs with different parameter sets:

(i) CRLP with $R_d=R$ and $|H|=1$;
(ii) CRLP with $|R_d|=\lceil r/3\rceil$ and $|H|=1$;
(iii) CRLP with $R_d=R$ and $|H|=3$;
(iv) CRLP with $|R_d|=\lceil r/3\rceil$ and $|H|=3$.

Note that when $|H|=1$, UAVs patrol at low altitude.

Furthermore, to assess the quality and robustness, we compare the solution of these four CRLPs with two patrol modes:

(i) Patrol mode of the average coverage strategy (ACS): UAVs are uniformly deployed in all zones. For each node $v=(i,t_k)$ of the directed graph G, the coverage of UAVs is $f(i,t_k)=m/r$.

(ii) Patrol mode of the probabilistic coverage strategy (PCS): UAVs are deployed according to the probability of detecting targets in each zone. A lower probability of detection in zone i corresponds to a higher coverage of the UAVs. For each node $v=(i,t_k)$ of the directed graph G, the coverage of UAVs is

$$f(i,t_k)=m\cdot\left(\sum_{k=1}^{T}(1-\delta(i,t_k))\right)\cdot\left(\sum_{k=1}^{T}\sum_{i=1}^{r}(1-\delta(i,t_k))\right).$$

The utility of the leader in the two patrol modes is obtained by the optimal choice of the follower against $\boldsymbol{f}$ in the two patrol modes.

5.2 Experimental evaluation

In this subsection, we analyze and evaluate the quality and robustness of CRLP and the scalability of DS-EM. The utility in the following subsections is the leader's optimal utility.

5.2.1 Solution quality

We first compare the solution quality among four CRLPs, ACS and PCS. Results are provided in Table 1. For each instance set, we present results of all instances when the number of UAVs is 20 in the first three rows, and the results of all given number of UAVs in all instances in the last three rows. The column PD-ACS is the percentage difference between the utility of CRLP and ACS. PD-PCS is the percentage difference between the utility of CRLP and PCS. The row Aver is the average percentage difference of the instances. Max is the maximum percentage difference of the instances. Min is the minimum percentage difference of the instances.

Table 1 Average results on utilities of four CRLPs, ACS, and PCS for all instances %

Set	UAV	Percentage difference	$R_d = R, \lvert H\rvert = 1$		$\lvert R_d\rvert = \lceil r/3\rceil, \lvert H\rvert = 1$		$R_d = R, \lvert H\rvert = 3$		$\lvert R_d\rvert = \lceil r/3\rceil, \lvert H\rvert = 3$	
			PD-ACS	PD-PCS	PD-ACS	PD-PCS	PD-ACS	PD-PCS	PD-ACS	PD-PCS
Set A	20	Aver	1.62	1.69	−0.05	0.02	5.08	5.14	4.88	4.95
		Max	3.75	3.70	0.08	0.20	11.07	10.99	10.73	10.75
		Min	0.70	0.74	−0.35	−0.43	2.28	2.32	2.17	2.22
	All	Aver	1.02	1.06	−0.03	0.01	3.20	3.24	3.08	3.12
		Max	3.75	3.70	0.08	0.20	11.07	10.99	10.73	10.75
		Min	0.18	0.19	−0.35	−0.43	0.58	0.58	0.55	0.56
Set B	20	Aver	2.63	3.03	−0.31	0.10	6.48	6.85	6.23	6.61
		Max	5.84	7.10	−0.11	0.68	13.83	14.98	13.32	14.42
		Min	1.14	1.30	−1.11	−0.42	2.86	3.07	2.80	2.90
	All	Aver	1.65	1.90	−0.19	0.10	4.10	4.34	3.94	4.18
		Max	5.84	7.10	−0.03	0.68	13.83	14.98	13.32	14.42
		Min	0.29	0.33	−1.11	−0.42	0.72	0.78	0.71	0.73
Set C	20	Aver	6.94	10.43	1.14	4.93	7.60	11.06	6.65	10.15
		Max	16.29	23.54	3.20	11.25	17.21	24.38	14.38	21.75
		Min	3.09	4.38	0.29	1.86	3.39	4.67	2.96	4.33
	All	Aver	4.42	6.67	0.71	3.11	4.82	7.05	4.20	6.46
		Max	16.29	23.54	3.20	11.25	17.21	24.38	14.38	21.75
		Min	0.78	1.11	0.07	0.47	0.86	1.19	0.75	1.10

Table 1 shows that, in general, CRLP has a greater advantage than ACS and PCS in utility with increasing number of UAVs. Specially, the leader has much higher utilities when the UAV can patrol at three altitudes without start and end zone limitations. The leader's utilities are lower when the number of start and end zones are limited to the minimum because the limitation of start and end zones reduces the leader's optional strategies. However, the utility of CRLP with $|R_d| = \lceil r/3\rceil$ and $|H| = 1$ is a little worse than that of ACS and PCS in some instances. The reason is that the patrol mode of ACS and PCS does not limit the start and end zones, so the zones that are not included in the start and end zones set are covered more at the start and end time points. In addition, PCS has the worst performance in most instances because the follower does not depend on only the detection probability when selecting his strategy.

To illustrate the effect of the number of zones, UAVs, and time points on leader's utilities, we present the results for Set A instances with the number of time points being six on Table 2 and Set C instances with the number of zones is 200 in Table 3. The column Inst, UAVs, Zone, and TP are the instance label, the number of UAVs, the number of zones, and the number of time points, respectively. The column PD-ACS is the average percentage difference between the utility of CRLP and ACS. PD-PCS is the average percentage difference between the utility of CRLP and PCS.

Table 2 Results on utilities of four CRLPs, ACS and PCS for Set A instances with six time points %

Inst	Zone	UAV	$R_d = R, \lvert H \rvert = 1$		$\lvert R_d \rvert = \lceil r/3 \rceil, \lvert H \rvert = 1$		$R_d = R, \lvert H \rvert = 3$		$\lvert R_d \rvert = \lceil r/3 \rceil, \lvert H \rvert = 3$	
			PD-ACS	PD-PCS	PD-ACS	PD-PCS	PD-ACS	PD-PCS	PD-ACS	PD-PCS
A01	200	5	0.95	0.90	−0.06	−0.11	2.89	2.84	2.72	2.67
		10	1.89	1.80	−0.12	−0.21	5.70	5.60	5.36	5.27
		15	2.83	2.69	−0.18	−0.32	8.42	8.29	7.93	7.79
		20	3.75	3.56	−0.23	−0.43	11.07	10.90	10.43	10.25
A07	400	5	0.48	0.48	−0.01	−0.02	1.46	1.46	1.38	1.38
		10	0.96	0.95	−0.03	−0.04	2.91	2.90	2.75	2.74
		15	1.44	1.42	−0.04	−0.06	4.33	4.31	4.09	4.08
		20	1.92	1.89	−0.06	−0.08	5.73	5.71	5.42	5.40
A13	600	5	0.32	0.33	0.00	0.00	0.98	0.98	0.92	0.93
		10	0.65	0.65	0.00	0.00	1.94	1.95	1.84	1.85
		15	0.97	0.98	0.00	0.01	2.90	2.91	2.75	2.76
		20	1.29	1.30	0.00	0.01	3.85	3.86	3.65	3.66
A19	800	5	0.24	0.24	−0.01	−0.02	0.73	0.73	0.68	0.68
		10	0.47	0.47	−0.03	−0.03	1.45	1.45	1.36	1.36
		15	0.71	0.71	−0.04	−0.05	2.17	2.16	2.03	2.03
		20	0.94	0.94	−0.06	−0.06	2.88	2.87	2.70	2.69
A25	1 000	5	0.19	0.20	−0.01	0.00	0.58	0.59	0.55	0.56
		10	0.38	0.39	−0.01	0.00	1.17	1.18	1.11	1.12
		15	0.57	0.59	−0.02	0.00	1.74	1.76	1.65	1.67
		20	0.76	0.79	−0.03	0.00	2.32	2.34	2.20	2.22

Table 3 Results on utilities of four CRLPs, ACS and PCS for Set C instances with 200 zones %

Inst	TP	UAV	$R_d = R, \lvert H \rvert = 1$		$\lvert R_d \rvert = \lceil r/3 \rceil, \lvert H \rvert = 1$		$R_d = R, \lvert H \rvert = 3$		$\lvert R_d \rvert = \lceil r/3 \rceil, \lvert H \rvert = 3$	
			PD-ACS	PD-PCS	PD-ACS	PD-PCS	PD-ACS	PD-PCS	PD-ACS	PD-PCS
C01	6	5	4.35	6.49	0.72	2.94	4.61	6.75	3.71	5.86
		10	8.50	12.56	1.43	5.79	9.01	13.04	7.28	11.38
		15	12.48	18.23	2.13	8.56	13.20	18.91	10.71	16.58
		20	16.29	23.54	2.83	11.25	17.21	24.38	14.02	21.47
C02	12	5	3.87	5.70	0.54	2.43	4.26	6.08	3.75	5.58
		10	7.60	11.08	1.09	4.81	8.34	11.79	7.36	10.85
		15	11.18	16.15	1.63	7.13	12.24	17.15	10.84	15.82
		20	14.62	20.93	2.16	9.39	15.98	22.18	14.18	20.52
C03	18	5	3.87	5.58	0.39	2.16	4.25	5.96	3.54	5.26
		10	7.59	10.85	0.77	4.28	8.33	11.57	6.96	10.25
		15	11.16	15.83	1.15	6.35	12.23	16.84	10.26	14.97
		20	14.60	20.53	1.53	8.37	15.96	21.80	13.44	19.45
C04	24	5	3.90	5.80	0.81	2.77	4.27	6.16	3.81	5.71
		10	7.65	11.26	1.61	5.46	8.35	11.94	7.47	11.09
		15	11.25	16.41	2.41	8.08	12.26	17.36	10.99	16.17
		20	14.72	21.26	3.20	10.63	16.01	22.45	14.38	20.95
C05	30	5	3.96	6.17	0.56	2.84	4.28	6.48	3.73	5.95
		10	7.76	11.95	1.11	5.60	8.37	12.54	7.33	11.54
		15	11.41	17.38	1.66	8.29	12.29	18.20	10.79	16.80
		20	14.92	22.48	2.21	10.89	16.05	23.50	14.12	21.75
C06	36	5	3.75	5.59	0.61	2.51	4.13	5.96	3.70	5.54
		10	7.35	10.86	1.21	4.96	8.08	11.56	7.27	10.78
		15	10.82	15.84	1.82	7.34	11.87	16.83	10.70	15.73
		20	14.16	20.54	2.41	9.67	15.51	21.79	14.01	20.40

Table 2 shows that with increasing number of UAVs, the leader's utilities of four CRLPs increase. This is consistent with the results in Subsection 4.3.2. When the number of zones increases, the utilities of leader decrease. It is surprising that there is not much reduction in leader's utilities when we limit the start and end zones. From another viewpoint, considering the actual patrols, the cost of UAV movement will be reduced because of certain start zones. In reality, the patrol is a continuous process. When there is no limit on the start and end zones, the ending zone of the UAV's last patrol may not be the starting zone of the next patrol. Therefore, limitation on start and end zones is needed when designing patrol strategy to ensure the continuity of patrols.

From Table 3, with increasing patrol duration, the utilities do not show the results in Subsection 4.3.2, since the detection probability between instances are not identical. When there is little difference between detection probabilities of different time spans, the gap between the utilities is small. Therefore, it is necessary to judge the gap of the detection probability between different time spans when deciding the patrol duration. Otherwise, a long-time patrol planning will lead to a significant reduction in utility.

Then, to further display how many UAVs are required to decrease the undetected probability to a certain extent, we compare the minimum number of UAVs required for four CRLPs when the undetected probability decreases to 0.2, 0.4, 0.6, and 0.8. Results are provided in Table 4 and Table 5. The columns Zone, Goal, and Inst are the number of zones, the expected undetected probability and the instance label, respectively. The last four columns are the average minimum number of UAVs required for four CRLPs.

Table 4 Average results on UAVs needed for four CRLPs for all instances

Zone	Goal	Inst	Minimum_UAV			
			$R_d = R, \|H\| = 1$	$\|R_d\| = \lceil r/3 \rceil, \|H\| = 1$	$R_d = R, \|H\| = 3$	$\|R_d\| = \lceil r/3 \rceil, \|H\| = 3$
200	0.2	A01-A06	232	317	148	151
		B01-B06	133	183	97	99
		C01-C06	67	93	65	68
	0.8	A01-A06	33	45	21	21
		B01-B06	19	26	14	14
		C01-C06	10	13	9	10
400	0.2	A07-A12	464	630	295	301
		B07-B12	266	362	194	198
		C07-C12	133	185	130	135
	0.8	A07-A12	65	88	42	42
		B07-B12	37	51	27	28
		C07-C12	19	26	18	19
600	0.2	A13-A18	696	951	443	452
		B13-B18	399	543	290	295
		C13-C18	200	260	194	204
	0.8	A13-A18	97	132	62	63
		B13-B18	56	76	41	41
		C13-C18	28	39	28	29
800	0.2	A19-A24	929	1 270	590	603
		B19-B24	531	726	387	394
		C19-C24	266	369	258	270
	0.8	A19-A24	129	176	82	84
		B19-B24	74	101	54	55
		C19-C24	37	51	36	38
1 000	0.2	A25-A30	1 160	1 584	737	754
		B25-B30	663	906	484	492
		C25-C30	332	460	323	338
	0.8	A25-A30	161	220	103	105
		B25-B30	93	126	68	69
		C25-C30	47	64	45	47

Table 5 Results on UAVs needed for four CRLPs for Set B instances

Inst	Zone	Goal	Minimum_UAVs			
			$R_d = R, \lvert H \rvert = 1$	$\lvert R_d \rvert = \lceil r/3 \rceil, \lvert H \rvert = 1$	$R_d = R, \lvert H \rvert = 3$	$\lvert R_d \rvert = \lceil r/3 \rceil, \lvert H \rvert = 3$
B01-B06	200	0.2	133	183	97	99
		0.4	76	104	56	57
		0.6	43	58	31	32
		0.8	19	26	14	14
B07-B12	400	0.2	266	362	194	198
		0.4	152	207	111	113
		0.6	85	115	62	63
		0.8	37	51	27	28
B13-B18	600	0.2	399	543	290	295
		0.4	227	309	166	169
		0.6	127	173	93	94
		0.8	56	76	41	41
B19-B24	800	0.2	531	726	387	394
		0.4	303	413	220	225
		0.6	169	231	123	125
		0.8	74	101	54	55
B25-B30	1 000	0.2	663	906	484	492
		0.4	378	516	276	281
		0.6	211	288	154	156
		0.8	93	126	68	69

Table 4 shows that UAVs are needed more for instances in Set A than that in Set B and Set C. Specially, when the undetected probability decreases to 0.2 for some instances in Set A, the number of needed UAVs is more than the number of zones. Thus, when the detection probability of UAVs is reduced to a certain extent, the cost of using UAVs to improve the probability of undetected is much higher. Corresponding to real patrols, when environmental factors greatly affect UAV detection probability, it may not be suitable to use UAVs to patrol.

Table 5 illustrates that more UAVs are needed with decreasing undetected probability and increasing number of zones. In addition, when the number of start and end zones is limited to the minimum and the UAVs patrol at a low altitude, the required number of UAVs is the highest, which is consistent with earlier results of utilities.

5.2.2 Robustness

In real life, the patrol strategy is planned in advance based on the leader's knowledge, but the real detection probability may deviate from the value in the previous setting due to climate fluctuations in the environment. In addition, the strategy that the follower observes may deviate from the leader's strategy due to the accuracy of the information. Therefore, we evaluate the robustness of our solution in two aspects:

(i) The detection probability of UAV $\hat{\delta}(v_h)$ in each vertex is in the range of $[(1-\alpha)\cdot\delta(v_h),(1+\alpha)\cdot\delta(v_h)]$.

(ii) The actual coverage of each vertex $\hat{f}_h(v_h)$ is in the range of $[(1-\beta)\cdot f_h(v_h),(1+\beta)\cdot f_h(v_h)]$, where α and β are the noises of the data.

Table 6 presents the results with $\alpha = 0.1$ and $\beta = 0.1$. For each instance set, we present results of all instances in the case of deviation of detection probability in the first three rows, and the results of all instances in the case of deviation of coverage in the last three rows. The row PDP-I, PDP-ACS, and PDP-PCS are the average percentage difference between the utility of CRLP in the case of deviation of detection probability and CRLP, ACS, and PCS, respectively. The row PDC-I, PDC-ACS, and PDC-PCS are the average percentage difference between the utility of CRLP in the case of deviation of coverage and CRLP, ACS, and PCS, respectively.

The percentage difference is $((\hat{U}_d - U_d)/(-U_d))\times 100$. In the case of deviation of detection probability, $\hat{U}_d$ is the utility of the leader obtained by the optimal choice of the follower against previous coverage $\boldsymbol{f}$ based on $\hat{\delta}$. In the case of deviation of coverage, $\hat{U}_d$ is the utility of the leader obtained by the optimal choice of the follower against $\hat{\boldsymbol{f}}$.

Table 6 Average results on robustness of four CRLPs compared with itself, ACS and PCS for all instances %

Set	Case	Percentage difference	$R_d = R, \lvert H\rvert = 1$	$\lvert R_d\rvert = \lceil r/3\rceil, \lvert H\rvert = 1$	$R_d = R, \lvert H\rvert = 3$	$\lvert R_d\rvert = \lceil r/3\rceil, \lvert H\rvert = 3$
Set A	Prop	PDP-I	−0.59	−0.43	0.02	0.06
		PDP-ACS	0.44	−0.46	3.22	3.14
		PDP-PCS	0.48	−0.42	3.26	3.18
	Cover	PDC-I	−0.40	−0.29	0.02	−0.04
		PDC-ACS	0.63	−0.32	3.22	3.04
		PDC-PCS	0.67	−0.28	3.26	3.08
Set B	Prop	PDP-I	−1.38	−0.97	0.00	0.21
		PDP-ACS	0.31	−1.16	4.10	4.13
		PDP-PCS	0.56	−0.90	4.34	4.37
	Cover	PDC-I	−0.70	−0.51	−0.02	0.21
		PDC-ACS	0.97	−0.70	4.08	4.14
		PDC-PCS	1.23	−0.44	4.32	4.38
Set C	Prop	PDP-I	−2.59	−1.33	−0.02	0.24
		PDP-ACS	1.99	−0.60	4.80	4.43
		PDP-PCS	4.32	1.84	7.04	6.68
	Cover	PDC-I	−1.38	−0.92	0.01	0.20
		PDC-ACS	3.14	−0.20	4.83	4.39
		PDC-PCS	5.44	2.23	7.06	6.65

From the results in Table 6, we can find that, in general, the solution of four CRLPs has strong robustness and performs better than ACS and PCS when the zone coverage and detection probability are uncertain. It also shows the stability of our solution in practical applications. Specifically, compared to the detection probability, the coverage has less influence on the solution quality. It is not surprising that a lower probability of detection corresponds to a smaller fluctuation of the solution. When the number of start and end zones of the UAV is limited to the minimum and the UAV patrols only at a low altitude, the utility is lightly worse than that of ACS and PCS in some instances. The reason is that the patrol mode of ACS and PCS do not limit the start and end zones, so the zones that are not included in the start and end zone sets are covered more at the start and end time points.

To further illustrate the fluctuation of solution in the case of two disturbances, we present the detailed results for Set C instance in Table 7 and Table 8. For each percentage difference, we present results of all instances when the number of UAVs is 20 in the first three rows, and the results of all given number of UAVs in all instances in the last three rows.

Table 7 Results in the case of deviation of detection probability for Set C instances %

PDP	UAV	Percentage difference	$R_d = R, \lvert H\rvert = 1$	$\lvert R_d\rvert = \lceil r/3\rceil, \lvert H\rvert = 1$	$R_d = R, \lvert H\rvert = 3$	$\lvert R_d\rvert = \lceil r/3\rceil, \lvert H\rvert = 3$
PDP-I	20	Aver	−3.92	−1.93	−0.02	0.28
		Max	−1.89	−0.43	0.36	1.73
		Min	−9.66	−3.52	−1.47	−0.88
	All	Aver	−2.59	−1.33	−0.02	0.24
		Max	−0.43	−0.14	0.57	2.09
		Min	−9.66	−4.83	−1.47	−1.48
PDP-ACS	20	Aver	3.34	−0.77	7.59	6.91
		Max	14.70	0.97	17.33	14.55
		Min	0.27	−2.38	3.39	2.19
	All	Aver	1.99	−0.60	4.80	4.43
		Max	14.70	1.23	17.33	14.55
		Min	0.02	−3.62	0.85	0.37
PDP-PCS	20	Aver	6.98	3.11	11.04	10.41
		Max	22.09	9.55	24.49	21.71
		Min	1.93	−0.34	4.84	3.49
	All	Aver	4.32	1.84	7.04	6.68
		Max	22.09	9.55	24.49	21.71
		Min	0.40	−0.40	1.28	0.88

Table 8 Results in the case of deviation of coverage for Set C instances

%

PDC	UAV	Percentage difference	$R_d = R, \lvert H\rvert = 1$	$\lvert R_d\rvert = \lceil r/3\rceil, \lvert H\rvert = 1$	$R_d = R, \lvert H\rvert = 3$	$\lvert R_d\rvert = \lceil r/3\rceil, \lvert H\rvert = 3$
PDC-I	20	Aver	−2.16	−1.49	0.12	0.35
		Max	0.00	−0.03	2.70	1.70
		Min	−5.09	−3.56	−0.97	−1.28
	All	Aver	−1.38	−0.92	0.01	0.20
		Max	0.00	0.00	2.70	1.70
		Min	−5.09	−3.56	−1.34	−1.76
PDC-ACS	20	Aver	4.99	−0.32	7.71	6.98
		Max	12.03	2.80	18.23	15.60
		Min	2.16	−1.84	2.97	2.92
	All	Aver	3.14	−0.20	4.83	4.39
		Max	12.03	2.80	18.23	15.60
		Min	0.53	−1.84	0.75	0.54
PDC-PCS	20	Aver	8.58	3.54	11.16	10.47
		Max	19.65	11.22	24.44	22.20
		Min	3.46	1.17	4.58	4.22
	All	Aver	5.44	2.23	7.06	6.65
		Max	19.65	11.22	24.44	22.20
		Min	0.88	0.29	1.25	1.02

Table 7 and Table 8 show that with increasing number of UAVs, the fluctuation of the solution becomes larger in both cases. However, the advantages of four CRLPs over ACS and PCS do not decrease and are more obvious, which also shows the stability of our solution in practical applications.

5.2.3 Scalability

In this subsection, we compare the efficiency of four CRLPs with and without the proposed DS-EM in Subsection 4.2. Results are presented in Table 9. For each instance set, we present results of all instances when the number of UAVs is 20 in the first three rows, and the results of all given number of UAVs in all instances in the last three rows. The column UAVs is the number of UAVs and IR-CPU is the percentage difference of runtime, which is computed as (CPU-CPU(DS-EM)/ CPU)×100. The row Aver is the average percentage difference of the instances. Max is the maximum percentage difference of the instances. Min is the minimum percentage difference of the instances.

Table 9 Average results on runtime of four CRLPs for all instances with and without DS-EM

Set	UAV	IR-CPU/%	$R_d = R, \lvert H\rvert = 1$	$\lvert R_d\rvert = \lceil r/3\rceil, \lvert H\rvert = 1$	$R_d = R, \lvert H\rvert = 3$	$\lvert R_d\rvert = \lceil r/3\rceil, \lvert H\rvert = 3$
Set A	20	Aver	72.32	60.05	82.26	84.50
		Max	96.40	89.07	98.06	98.89
		Min	37.33	9.76	22.49	12.26
	All	Aver	73.33	61.38	81.56	84.99
		Max	97.13	90.74	98.06	98.95
		Min	17.84	9.76	18.67	2.16
Set B	20	Aver	76.24	57.83	82.83	84.79
		Max	96.56	87.21	97.15	98.69
		Min	27.98	5.66	21.49	35.57
	All	Aver	74.73	59.59	84.64	84.14
		Max	96.89	91.22	97.52	98.82
		Min	6.57	5.66	18.86	17.70
Set C	20	Aver	80.33	72.75	81.23	82.37
		Max	98.26	90.55	97.16	98.66
		Min	45.19	45.87	18.71	1.81
	All	Aver	79.42	70.53	80.20	83.23
		Max	98.26	90.73	97.16	98.86
		Min	35.63	24.81	9.41	1.81

Table 9 shows that the proposed DS-EM greatly improves the solution efficiency. Consistent with our thought, the runtime decreases when the start and end zones are limited and increases when the number of patrol altitudes increases. Further, the time is required more when the UAV can patrol at three altitudes and limit the start and end zones, because variables and constraints increase when limiting start and end zones.

To illustrate the effect of the number of zones and time points on runtime, we present the results for Set A instances with the number of time points is 24 in Table 10 and Set B instances with the number of zones is 600 in Table 11. The columns Inst, Zone, and TP are the instance label, the number of zones, and the number of time points, respectively. The last four columns are the average percentage difference of the instances.

Table 10 Results on runtime of four CRLPs for Set A instances with 24 time points %

Inst	Zone	IR-CPU			
		$R_d = R, \lvert H\rvert = 1$	$\lvert R_d\rvert = \lceil r/3\rceil, \lvert H\rvert = 1$	$R_d = R, \lvert H\rvert = 3$	$\lvert R_d\rvert = \lceil r/3\rceil, \lvert H\rvert = 3$
A04	200	90.50	86.86	92.61	93.10
A10	400	91.54	85.78	97.75	96.87
A16	600	66.13	86.45	96.41	96.25
A22	800	61.65	84.55	96.59	95.96
A28	1 000	86.80	88.62	95.36	95.71

Table 11 Results on runtime of four CRLPs for Set B instances with 600 zones %

Inst	TP	IR-CPU			
		$R_d = R, \lvert H\rvert = 1$	$\lvert R_d\rvert = \lceil r/3\rceil, \lvert H\rvert = 1$	$R_d = R, \lvert H\rvert = 3$	$\lvert R_d\rvert = \lceil r/3\rceil, \lvert H\rvert = 3$
B13	6	58.90	51.49	39.41	52.09
B14	12	72.19	66.85	89.45	64.33
B15	18	80.98	75.89	94.61	96.57
B16	24	81.36	79.93	95.17	94.83
B17	30	85.46	45.58	95.60	94.79
B18	36	86.17	36.93	95.46	94.58

Table 10 and Table 11 illustrate that, in general, compared to the increase in number of zones, the DS-EM is more efficient in increasing the time duration because the DS-EM greatly reduces the number of pure strategies of the follower in the time dimension.

6. Conclusions

In this paper, the problem of deploying UAVs on borders is modeled as a leader-follower Stackelberg game with the aim to find an effective patrol strategy to detect the illegal immigrant. The objective of the leader is to determine the optimal patrol path of UAVs under different patrol altitudes. The follower selects a time and area with the minimum probability of being detected to cross the border after observing the leader's strategy. To ensure the continuity of the actual patrol, UAVs are limited to starting and ending their patrols in certain zones. However, such limitations make some strategies invalid. Conditions for effective leader's strategy are developed to provide a preliminary intuition for decision makers. In addition, some properties of leader's utilities are stated to help the border patrol agency make a trade-off between costs and utilities.

With the increase in scale of the game, the number of strategies of the leader exponentially increases with time and space. To solve the computational challenge, first, a nonlinear programming model in a compact form named CRLP is proposed to reduce the variables in the original model. Then, the constraints for the follower are linearized to build an equivalent model. When the time and space increase, the strategy space of the follower rapidly grows. Therefore, we propose a method named DS-EM to reduce the strategy space of the follower by eliminating the strategies that are not performing well.

To evaluate the solution quality and robustness, we compare the solution in four CRLPs that have different parameter sets with two conventional patrol strategies on generated instances. The computational results show that the proposed solution has better utilities than the two strategies, and is able to provide an effective patrol strategy to detect illegal entry and secure the border. Moreover, the proposed solution is strongly robust when the zone coverage and detection probability are disturbed. The performance of the DS-EM is assessed on four CRLPs. The experimental results show that the elimination method can significantly improve the efficiency. In the future, we will focus on exploring new ideas of strategy reduction and designing an effective patrol strategy under uncertain situations, e.g., the time required for the follower to cross different areas along the border is uncertain.

References

[1] SECURITY H. Border security results. https://www.dhs.gov/border-security-results.

[2] PROTECTION U C A B. 2020 U.S. border patrol strategy. https://www.cbp.gov/border-security/along-us-borders/strategy.

[3] LINEBARGER C, BRAITHWAITE A. Do walls work? The effectiveness of border barriers in containing the cross-border spread of violent militancy. International Studies Quarterly, 2020, 64(3): 487–498.

[4] JORDAN S, MOORE J, HOVET S, et al. State-of-the-art technologies for UAV inspections. IET Radar, Sonar & Navigation, 2018, 12(2): 151–164.

[5] GUO S, XIONG X X, LIU Z C, et al. Infrared simulation of large-scale urban scene through LOD. Optices Express, 2018, 26(18): 23980–24002.

[6] ZHOU R H, SUN H M, LI H, et al. TDOA and track optimization of UAV swarm based on D-optimality. Journal of Systems Engineering and Electronics, 2020, 31(6): 1140–1151.

[7] FRONTEX. Frontex R&D UAV workshop and Demo 2011 - call for expressions of interest. https://frontex.europa.eu/future-of-border-control/research-and-innovation/announcements/frontex-r-d-uav-workshop-and-demo-2011-call-for-expressions-of-interest-EDouHq.

[8] CASORRAN C, FORTZ B, LABBE M, et al. A study of general and security Stackelberg game formulations. European Journal of Operational Research, 2019, 278(3): 855–868.

[9] PITA J, JAIN M, MARECKI J, et al. Deployed ARMOR protection_the application of a game theoretic model for security at the Los Angeles International Airport. Proc. of the 7th International Conference on Autonomous Agents and Multiagent Systems, 2008: 125–132.

[10] TSAI J, RATHI S, KIEKINTVELD C, et al. IRIS-a tool for strategic security allocation in transportation networks. Proc. of the 8th International Conference on Autonomous Agents and Multiagent Systems, 2009: 37–44.

[11] PITA J, TAMBE M, KIEKINTVELD C, et al. GUARDS-game theoretic security allocation on a national scale. Proc. of the 10th International Conference on Autonomous Agents and Multiagent Systems, 2011: 37–44.

[12] MUAAFA M, RAMIREZ-MARQUEZ J E. Bi-objective evolutionary approach to the design of patrolling schemes for improved border security. Computers & Industrial Engineering, 2017(107): 74–84.

[13] BUCAREY L V, CASORRAN C, LABBE M, et al. Coordinating resources in stackelberg security games. European Journal of Operational Research, 2021, 291(3): 846–861.

[14] KARABULUT E, ARAS N, KUBAN ALTıNEL I. Optimal sensor deployment to increase the security of the maximal breach path in border surveillance. European Journal of Operational Research, 2017, 259(1): 19–36.

[15] LESSIN A M, LUNDAY B J, HILL R R. A bilevel exposure-oriented sensor location problem for border security. Computers & Operations Research, 2018, 98: 56–68.

[16] BAYKAL-GURSOY M, DUAN Z, POOR H V, et al. Infrastructure security games. European Journal of Operational Research, 2014, 239(2): 469–478.

[17] YOLMEH A, BAYKAL-GURSOY M. A robust approach to infrastructure security games. Computers & Industrial Engineering, 2017, 110: 515–526.

[18] JIE Y M, LIU C Z, LI M C, et al. Game theoretic resource allocation model for designing effective traffic safety solution against drunk driving. Applied Mathematics and Computation, 2020, 376: 125142.

[19] SHIEH E, AN B, YANG R, et al. PROTECT: a deployed game theoretic system to protect the ports of the United States. Proc. of the 11th International Conference on Autonomous Agents and Multiagent Systems, 2012: 13–20.

[20] PAULSON E C, LINKOV I, KEISLER J M. A game theoretic model for resource allocation among countermeasures with multiple attributes. European Journal of Operational Research, 2016, 252(2): 610–622.

[21] GOLANY B, GOLDBERG N, ROTHBLUM U G. A two-resource allocation algorithm with an application to large-scale zero-sum defensive games. Computers & Operations Research, 2017, 78: 218–229.

[22] CANBOLAT M S, WESOLOWSKY G O. A planar single facility location and border crossing problem. Computers & Operations Research, 2012, 39(12): 3156–3165.

[23] BASILICO N, GATTI N, AMIGONI F. Patrolling security games: definition and algorithms for solving large instances with single patroller and single intruder. Artificial Intelligence, 2012, 184/185: 78–123.

[24] YIN Z Y, JIANG A X, TAMBE M, et al. Trusts: scheduling randomized patrols for fare inspection in transit systems using game theory. AI Magazine, 2012, 33(4): 59–72.

[25] BASILICO N, GATTI N, AMIGONI F. Leader-follower strategies for robotic patrolling in environments with arbitrary topologies. Proc. of the 8th International Conference on Autonomous Agents and Multiagent Systems, 2009: 57–64.

[26] ALPERN S, MORTON A, PAPADAKI K. Patrolling games. Operations Research, 2011, 59(5): 1246–1257.

[27] ALPERN S, LIDBETTER T, PAPADAKI K. Optimizing periodic patrols against short attacks on the line and other networks. European Journal of Operational Research, 2019, 273(3): 1065–1073.

[28] PAPADAKI K, ALPERN S, LIDBETTER T, et al. Patrolling a border. Operations Research, 2016, 64(6): 1256–1269.

[29] SARICICEK I, AKKUS Y. Unmanned aerial vehicle hub-location and routing for monitoring geographic borders. Applied Mathematical Modelling, 2015, 39(14): 3939–3953.

[30] GIRARD A R, HOWELL A S, HEDRICK J K. Border patrol and surveillance missions using multiple unmanned air vehicles. Proc. of the IEEE 43rd Conference on Decision and Control, 2004: 620–625.

[31] AMANATIADIS A, BAMPIS L, KARAKASIS E G, et al.

Real-time surveillance detection system for medium-altitude long-endurance unmanned aerial vehicles. Concurrency and Computation: Practice and Experience, 2018, 30: e4145.
[32] KIM S J, LIM G J. Drone-aided border surveillance with an electrification line battery charging system. Journal of Intelligent & Robotic Systems, 2018, 92(3/4): 657–670.
[33] ZHANG Y, YUAN X X, LI W Z, et al. Automatic power line inspection using UAV images. Remote Sensing, 2017, 9(8): 824–842.
[34] ZHOU H L, KONG H, WEI L, et al. On detecting road regions in a single UAV image. IEEE Trans. on Intelligent Transportation Systems, 2017, 18(7): 1713–1722.
[35] XU J W, DENG Z H, SONG Q, et al. Multi-UAV counter-game model based on uncertain information. Applied Mathematics and Computation, 2020, 366: 124684.
[36] BASILICO N, CARPIN S. Online patrolling using hierarchical spatial representations. Proc. of the IEEE International Conference on Robotics and Automation, 2012: 2163–2169.
[37] BASILICO N, CHUNG T H, CARPIN S. Distributed online patrolling with multi-agent teams of sentinels and searchers. Proc. of the International Symposium on Distributed Autonomous Robotic Systems, 2014: 3–16.
[38] BASILICO N, DE NITTIS G, GATTI N. Adversarial patrolling with spatially uncertain alarm signals. Artificial Intelligence, 2017, 246: 220–257.
[39] KHANDUZI R, MALEKI H R. A novel bilevel model and solution algorithms for multi-period interdiction problem with fortification. Applied Intelligence, 2017, 48(9): 2770–2791.
[40] YIN Y, AN B. Efficient resource allocation for protecting coral reef ecosystems. Proc. of the 25th International Joint Conference on Artificial Intelligence, 2016: 531–537.
[41] KIEKINTVELD C, JAIN M, TSAI J, et al. Computing optimal randomized resource allocations for massive security games. Proc. of the 8th International Conference on Autonomous Agents and Multiagent Systems, 2009: 689–696.

Biographies

LEI Xing was born in 1994. She received her B.S. degree from Hefei University of Technology in 2016. She is currently pursuing her Ph.D. degree in the School of Management, Hefei University of Technology. Her current research interests include deploying multi-UAVs for border patrols and security game theory.
E-mail: leixing@mail.hfut.edu.cn

HU Xiaoxuan was born in 1978. He received his B.S. and Ph.D. degrees from Hefei University of Technology, in 1999 and 2006, respectively. He is a professor in Hefei University of Technology. His current research interests include satellite mission planning, unmanned system intelligence, and aerospace system management.
E-mail: xiaoxuanhu@hfut.edu.cn

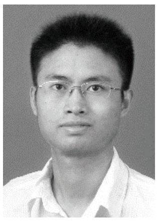

WANG Guoqiang was born in 1982. He received his B.S. and M.S. degrees from University of Science and Technology of China, in 2004 and 2007, respectively. He received his Ph.D. degree from Hefei University of Technology in 2016. He is a professor in Hefei University of Technology. His current research interests include management and intelligent decision making of unmanned aerial vehicle formation.
E-mail: gqwang2017@hfut.edu.cn

LUO He was born in 1982. He received his B.S. and Ph.D. degrees from Hefei University of Technology, in 2004 and 2009, respectively. He is a professor in Hefei University of Technology. His current research interests include intelligent decision making, multi-agent system, and the applications of unmanned aerial vehicle.
E-mail: luohe@hfut.edu.cn